EurJIC
European Journal of Inorganic Chemistry

A Journal of
ChemPubSoc Europe

Accepted Article

Title: Fabrication of flower like Ag microspheres film with its application in catalysis and as SERS substrates

Authors: Qijun Dai, Lu Li, Chungang Wang, Changli Lv, Zhongmin Su, and Fang Chai

To be cited as: *Eur. J. Inorg. Chem.* 10.1002/ejic.201800119

Link to VoR: http://dx.doi.org/10.1002/ejic.201800119

WILEY-VCH

Fabrication of flower like Ag microspheres film with its application in catalysis and as SERS substrates

Qijun Dai,[a,b], Lu Li,[a] Chungang Wang, [a] Changli Lv, * [a] Zhongmin Su* [a] and Fang Chai* [a,b]

Abstract: Three-dimensional flower like Ag microstructures were assembled in situ on the substrate to fabricate Ag micro-flower (Ag MFs) film. The morphology and size of the Ag structures of these Ag MFs can be easily controlled by varying reaction time. And the mechanism of growth of Ag MFs was also investigated by SEM. The shape evolution revealed the Ag MFs was assembled with thin nanosheets which composed of Ag nanoparticles, and the elemental composition of the nanoparticles was evidenced by X-ray spectroscopy analysis. Its potential which used as a catalyst in the reaction of reduction of nitrophenols was investigated. The reusability of the catalyst of the Ag MFs film was also estimated by recycling catalysis of 4-nitrophenol. Moreover, the Ag MFs film could be used as a versatile Surface Enhanced Raman Scattering (SERS) substrate for detection of the R6G molecules with a detection limit as low as 1×10^{-7} M. The results demonstrate that the Ag MFs film exhibit excellent SERS enhancement ability and catalytic activity.

Introduction

Large-scale production of metallic nanocrystals have attracted great attention due to their fascinating size- and shape-dependent properties for various applications, such as catalysis, sensing, plasmonics and photothermal therapy.[1] In particular, the significant efforts have promoted the development of the shape controlled synthesis of silver nanoparticles in past decades.[2-7] The synthesis of the Ag particles with different shapes and sizes are currently widely investigated due to shape control shows a greater versatility for tuning the properties of the Ag nanostructures. So, tremendous efforts have been made to search for a versatile method to precisely control the morphology of Ag NPs over the past decade, due to the application such as catalyst can be strongly affected by particle size and shape.[2,5,7,8] Recently, a class of sophisticated attractive structures of Ag has been synthesized by electrochemical method, chemical deposition method, galvanic replacement and so on. [8] For example, Nie and co-workers reported flower-like silver hierarchical microcrystals through reducing silver nitrate by L-ascorbic acid in nitric acid-mediated systems with high catalytic activity.[9] Xu' s group designed a kind of porous Ag platelet structures and exhibited excellent catalytic activity.[10] Chang and co-workers fabricated a thin Ag film into nanocrystals (NCs) with various shapes including nanoflowers by cyclic scanning electrodeposition method.[11] And You's group prepared a rose-like Ag mesoparticles on screen-printed carbon electrode using cyclic voltammetric methods, which was use as surface-enhanced Raman scattering substrate.[12] Pillai and co-workers presented a facile synthetic approach that involves the use of sustainable nanocellulose for the synthesis of flower-like Ag nanostructure with optical properties.[13] Among them, flower like structure of Ag particle which was usually assembled by nano- or submicro-plates was one of most remarkable materials in all reported Ag structures due to its highly branched structures, large specific surface area and rough surface. There are a large number of reports on the synthesis of flower like Ag nan- micro-structure with their excellent applications in catalysis, biological labeling, chemical sensing, electrocatalysis, SERS detection and so on.[3, 14-17]

However, mostly used various surfactants during the controllable preparation inevitably blight the activity of Ag NPs used as catalysts, substrates and assembling units. Therefore, the shape-, size-controllable synthesis on the large scale is still a significant challenge, especially under the mild condition of without any additive surfactants. Furthermore, the sustainable reuse of the noble metal materials is strongly advocated due to the cost of noble metals is one of the key limitations for their practical application.[18] The recovery of expensive catalysts after catalytic reactions and reusing them without the loss of activity are essential features for sustainable process development.[19] To improve the efficiency and save resources, the possible solution is of urgent need to exploit. Nevertheless, there are only two more effective way including the use of magnetically retrievable Ag nanoparticles[20] and fabricating the large scale Ag surface on substrate.

The fabrication of nanostructured metal surfaces (such as Au and Ag) [21] can be treated as a efficacious process in efficient green chemical synthesis, which could provide outstanding applications in recyclable heterogeneous catalysis, biological labeling, SERS and electrocatalysis.[11,22,23] Though, fabricating the silver microcrystals in large-scale is of scientific significance, greatly underdeveloped as the lack of rational design strategies, which meaning that the applications of these desirable superstructures remain limited because of the complexity of their synthesis or low yield during fabrication.[1,11,12]

Stimulated by this, we have synthesized flower like Ag microstructures and assembled in situ on the substrate to fabricate Ag micro-flower (Ag MFs) film by a low cost and facile synthetic route, a two-step process seed-assisted auto-catalytic reaction. To investigate the catalytic activity of the Ag MFs, the hydride reduction from 4-nitrophenol (4-NP) to 4-aminophenol (4-AP) by $NaBH_4$ is used as a model reaction, due to the process of reaction can be monitored by ultraviolet–visible absorption spectroscopy. And more importantly, it is of great significant to produce the 4-AP from reduction of the 4-NP, owing to 4-NP is the most ordinary organic pollutant and

---

[a] Qijun Dai, Lu Li, Chungang Wang, Changli Lv, Zhongmin Su and Fang Chai
Institute of Functional Material Chemistry, Faculty of Chemistry
Northeast Normal University
Changchun, 130024, P.R. China
E-mail: lucl055@nenu.edu.cn, zmsu@nenu.edu.cn
[b] Qijun Dai, Fang Chai
Faculty of Chemistry
Harbin Normal University
Harbin, 150025, P.R. China
E-mail: fangchai@gmail.com

Supporting information for this article is given via a link at the end of the document.

carcinogenic to humankind and wildlife, while its amino derivative, 4-AP is an important intermediate for the manufacture of analgesic and antipyretic drugs.[18,19, 24] In this work, the Ag MFs film exhibit excellent catalytic activity and reusability for the reduction of nitrophenols in aqueous solution. Compared with reported method, this method can be regarded as a feasible and sustainable method for reuse the noble metal.

Otherwise, as we know, the Surface-enhanced Raman scattering (SERS) by using the Ag clusters or aggregated has been demonstrated as a powerful tool for ultrasensitive chemical detection.[12,13,25-27] As mentioned previously, flower-like Ag particles have a unique morphology and rough surface, rendering them suitable active substrates for SERS. And a class of sophisticated flower-like Ag structures with different sizes are currently widely investigated for developing a highly efficient SERS substrate.[15-17] So, in this work, the Ag MFs film is also attempt to using as SERS substrate for detection of R6G.[26]

Results and Discussion

The fabrication of the Ag MFs film was a two steps process, the seeds fastened on the substrate and grew in the Ag^+ solution. By immersing in the APTMS solution, the glass and silicon slices were pretreated by the $-NH_2$. In succession, the substrate was soaked in 15 nm Au NPs (Fig. S1) to stick the Au NPs as seeds by $-NH_2$ decorated on the substrates. These seeds are necessary to obtain well-ordered flower-like Ag sturctures and well-dispersed on the substrate. The gold nanoseeds modified substrate was then immersed in the Ag^+ solution with the hydroquinone at low pH. The Ag nanoflowers were emerged sited on the seeds quickly by the seed-assisted auto-catalytic reaction, which can be tuned to create a huge variety of nanoparticle morphologies. [28] The large field Ag NFs assembled to well-distributed Ag film.

The FE-SEM images revealed that the morphology of the Ag MFs film were assembled uniformly by a large number of spherical flower like structure with a rough surface by this simple method. The Ag MFs film formed by 3 min (Fig. 1a) and 8 min (Fig. 1d) were presented in a larger field of view. As can be seen from the Fig. 1a-c, the large scale equidistribution of silver flower was produced within 3 min. The spherical flower-like Ag nanostructures have been formed with the diameter of 150-200 nm. And most of them were assembled by large scale fan-shape thin Ag nanosheet with thickness of 20 nm. As can be observed (Fig. 1b), the semicircle petals were assembled by single flabellate lamellar nanosheets by across each other with the diameter of 100-150 nm. It seems that the Ag nanosheets were at the initial stage of assembling, but the flowerlike structures have already been recognizable. More accurately, as can be detected from the sparse petals in Fig. 1c, the assembled lamellar nanosheets were composed of the dendritic silver nanoparticles. These results indicated that the Ag flower structures were formed within 3 min preliminarily. The Ag nanosheets composed of flower structure were expanded by Ag nanoparticles extending dendritic growth. Though most of Ag nanosheets accumulated together, the process of growth and self-assembling was still in progress. When the reaction was finished at 8 min, the Ag flower structure of film was pronounced in large domains, and longer reaction time seems in favor of the growth of Ag MFs structure. The Fig. 1d presents that the large scale film was assembled by independent Ag flowers with the diameter of 300-450 nm. The highly branched Ag microflower formed which enlarged twice than the reaction at 3 min. The sparse petals can be observed folded by several layer of intercrossed nanosheets (Fig. 1e). The thinness of Ag nanosheet was still remained at about 20 nm, but the growth proceeded along the dendritic direction (Fig. 1f, Fig. S2). The Ag NPs which arranged in a dendritic Ag thin nanosheet, were clearly visible with the diameter of 30-50 nm. Accompany the increase of reaction time, the Ag nanosheets grew about twice bigger gradually at the cost of little particles.[27] The EDS measurements further confirmed the Ag MFs film respectively (Fig. S3a and S3b), and proved the existence of only Ag atoms without Au atoms. This result indicated that the Au nanoseeds were used as precursor to fabricate a nanosheets-assembled Ag flower-like structure by seed-assisted auto-catalytic reactions.[29]

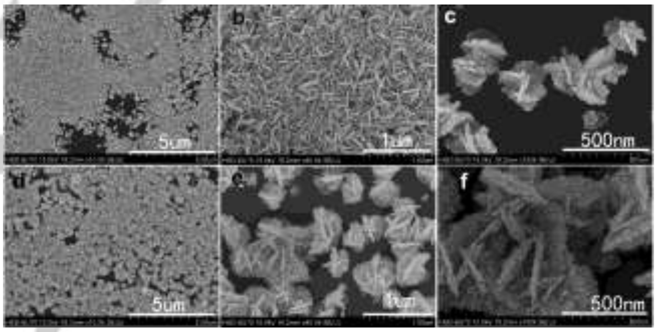

Figure 1. SEM images of Ag MFs film with different reaction time (a, b and c: 3 min, d, e and f: 8 min).

The TEM was used to evaluate the morphology of the Ag micro flower which was peeled off from the substrate. The single Ag MF was a spherical shape (Figure 2a) with diameter of around 1.2 μm, and the flimsy nanosheet at the edge (Figure 2b) can be observed clearly, indicating that the flower consisted of a lot of nanosheets, which were consistent with those observed under SEM investigation. And through extensive investigation by selected area electron diffraction (SAED), we found that the subunits of Ag MFs single layer Ag nanosheets exhibited single crystalline nature. The high-resolution TEM (HRTEM) image of the nanosheet at the edge of flower was shown in Fig. 2c, which depicted the continuous lattice fringes in the visible range, indicating its single crystal-line nature. And clear lattice structure of the Ag nanosheet can be seen, the lattice spacing was measured to be about 0.23 nm (inset of Fig. 2c), which matched the interplanar distance of the (111) planes of Ag face-centered cubic (fcc) structure. The chemical compositions of Ag MF were determined by energy dispersive X-ray (EDS) (Fig. 2d), which proved the presence of the Ag element, and other peaks originated from the copper and carbon from the TEM grid.

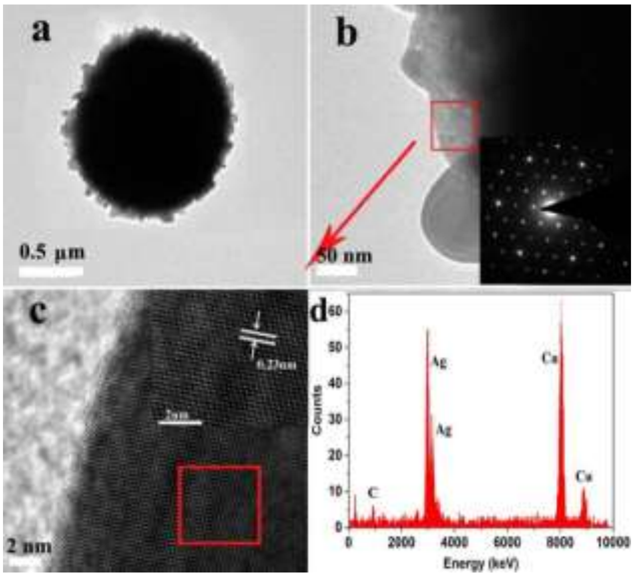

Figure 2. TEM of the Ag microflower a. the edge of the flower, b. the nano sheet of the edge of Ag flower (inset: SEAD pattern of Ag nanosheet), c. HRTEM images of single layer of Ag nano sheet with lattice parameters of 0.23 nm (inset), d. EDS of the Ag MFs.

In order to understand the morphological evolution of the Ag MFs film, the growth was monitored by different reaction time, and the structures grown at different stages were examined by SEM. When the reaction started, the spherical Ag nanoparticles were produced through seed-mediated growth immediately and spread on the substrate uniformly in a large scale (Fig. 3a). The Ag NPs were formed by reducing on the embedded Au nano beads with smooth surface and a diameter of 100-120 nm (inset of Fig. 3a). The precipitation speed of Ag NPs was appropriate, at which nanosheets can be obtained and then assembled into 3D architectures (Fig. 3b). Obviously, with the increase of reaction time, the surface roughness of Ag NPs increased, since the growth and aggregation of Ag nanosheets became faster, which was much faster than Ostwald ripening Au seeds sacrificed smaller crystallites, finally led to the rough surface of silver particles by aggregation grown (Fig. 3b-d). [9, 29]

With the addition of the reaction time, the single layer of Ag nano sheets were assembled to aggregated sheets (Fig. 3c). Fig. 3d shows the typical FESEM image of Ag MFs film, in which a nanosheet-assembled flower-like structure with the size of 400-600 nm can be seen. The resulted highly branched Ag MFs structure evoluted accompanied reaction time, the process of formation was highly reproducible. Based on these findings, it can be deduced that the size and shape of Ag nanoparticles are highly dependent on the reaction time at milder reducing conditions. The growth of flower structure was clearly observable as the seed-assisted auto-catalytic reaction was still proceeded. The distinct flower-like framework possessing the largest surface area produced after 3 min, and the absolute Ag MFs film can be fabricated within 8 min, potentially making subsequent seed-assisted auto-catalytic reaction more efficient for construction of subsequent nanostructures. [30] And it needs to be pointed out that the amount of Au NPs loading on the substrate can affected the growth of the Ag MFs film. The Ag MFs films with the substrate soaking different time in Au NPs were compared in Fig. S4. The less Au NPs loading on the substrated resulted in the inadequacy growth of the Ag MFs, while the redundant soakin led to the big block on the film. Thus the optimized soaking time was determined at 10-15 min.

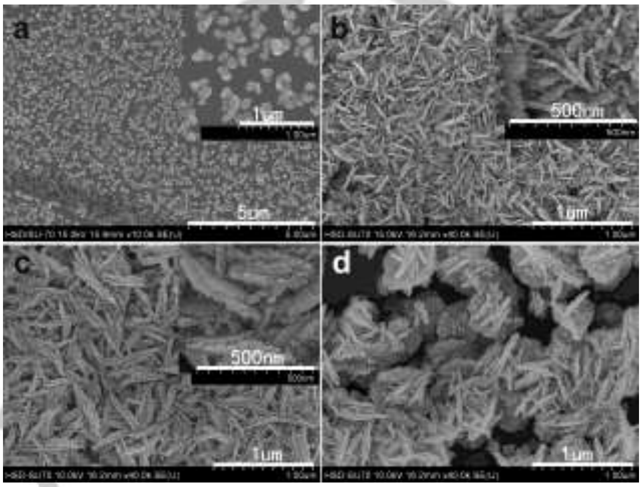

Figure 3. SEM image of shape evolution of the Ag MFs film with increasing duration of reaction (a.1 min, b.3 min, c.5 min, d.8 min)

The catalytic activity of Ag MFs film was tested as heterogeneous catalysis catalyst by a model reaction reduction of nitrophenol to aminophenol, due to the catalytic hydrogenation of nitrophenol by noble metal particles was considered as a green process.[9, 24, 30-33] The time resolutions of the kinetic measurements were limited by the integration times for UV-vis spectra collection. Firstly, the reduction of 4-nitrothiophenol (4-NTP) was first tested by using Ag MFs film as a catalyst. It is clear to be seen that the yellow fading and eventual bleaching, during the catalytic reactions, the complete hydrogenation of 4-NTP into 4-aminothiophenol (4-ATP) has been occurred. Fig. 4 reveals the successive UV-visible (UV-vis) absorption spectra for the 4-NTP can be transferred to 4-ATP catalyzed by Ag MFs film within 10 min exhibiting the high activities. As the catalytic reaction proceeds, the absorption peak at 410 nm originating from 4-NTP gradually decreases, indicating the continuous reduction of 4-ATP. To estimate the efficiency of the catalyst, the predetermined calibration curve has been confirmed in Fig. S5. And to give a quantitative description about the catalytic performance, the apparent rate constant of the reducing reaction was calculated. Since $NaBH_4$ is far excessive for the concentration of 4-NTP, reaction kinetics is independent of $NaBH_4$ concentration, it is reasonable to regard the concentration of $NaBH_4$ as a constant throughout the reaction. Thus, the reduction kinetics can be conformed to be pseudo-first-order kinetics.[34] As shown in the inset of $\ln(C_t/C_0)$ exhibits a linear relationship with the reaction time. The apparent rate constants was calculate to 0.2166 min^{-1} (R^2=0.9879). As is well known, the 4-NTP is more difficult to reduction than 4-NP due to the existence of the structure of –SH, which indicated the good catalytic activity of Ag MFs film. Owing to the high surface areas of Ag MFs, which favouring to the interactions between the reactants and the catalyst surface. And the stability of Ag MFs film was also evaluated by SEM and EDS after the use of catalyst, due to the property of metal nanoparticles exhibited strongly dependent on their size, shape, morphology and composition.[11] As revealed by the SEM (Fig. S6), the Ag MFs film still remained the flower structure after the splashing by the solution in the reaction, which was ensured the high surface areas and favor to improve the catalytic activity. And the EDS manifested that the main element was still Ag element, indicated the good stability of the Ag MFs film, which permitted the utility as a catalyst in a next turn.

The Ag MFs were fabricated on the substrate which provided a feasibility of recycle. The Fig. 5 illustrates the recyclable usage of the Ag MFs film in the reaction of reduction of 4-NP. The reusability of Ag MFs film was investigated in detail by using it as catalyst in recycle reactions of reduction of 4-NP. The original 4-NP solution was light yellow with a maximum absorption at 317 nm, which could not be reduced by $NaBH_4$ without catalyst. After adding the aqueous solution of $NaBH_4$, the formation of 4-nitrophenolate anions caused the maximum absorption to shift to about 400 nm (Fig. S7, S8). Meanwhile, the absorbance at 300 nm related to aminophenol slightly increased and led to a small peak there. As demonstrated in the Fig.5, the 4 successive reduction cycles were performed using a slice of Ag MFs film fabricated on glass as the catalyst. As revealed in Fig. 5a and b, 100% reduction of 4-NP was achieved within 12 min in the first two cycles with the kinetic rate constants of 6.54×10^{-3} s^{-1} and 4.47×10^{-3} s^{-1} respectively. However, the latter two cycles, more than 97% 4-NP were reduced within 14 and 18 min with the kinetic rate constants of 3.38×10^{-3} s^{-1} and 2.61×10^{-3} s^{-1} respectively (Fig. 5c and d). These results suggest that the Ag MFs film can be successfully recycled for at least 4 successive cycles with a stable conversion efficiency of around 97 % (Fig. 5e and inset).

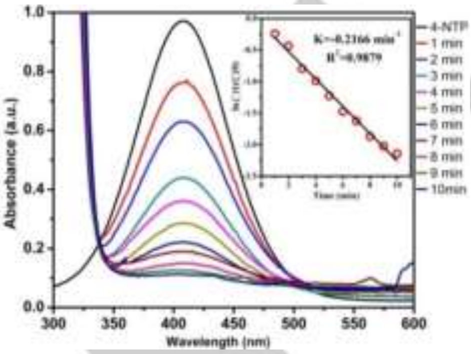

Figure 4. The absorption spectra of catalytic reduction of 4-NTP to 4-ATP by fresh solution of $NaBH_4$ in the presence of Ag MFs film as catalyst. (Inset: The plot of ln(C(t)/C(0)) versus reaction time for the reduction of 4-NTP.)

To evaluate SERS performance, the R6G was selected as the model SERS probe, due to its large cross section and well-characterized Raman bands. As revealed in Fig. 6a, all the feature peaks of R6G at 1646, 1570, 1533, 1504, 1356, 1311, 1186, 769 and 606 cm^{-1} were observed and consistent with other research studies, and peaks of R6G at 1186, 1311, 1356, 1504, and 1646 cm^{-1} were observed and assigned to C–H in-plane bending, C–O–C stretching, and C–C stretching of the aromatic ring.[14] However, the Ag NPs (Fig. 3a, prepared by the process of the fabrication of the Ag MFs) showed very weak SERS ability (black curve), the SERS activity of petals of Ag MFs was enhanced a lot (red curves), which indicated the Ag petals improved the SERS signal of R6G. This clearly shows the ability of the Ag MFs film to enhancing the detection sensitivity. And Fig. 6b shows the SERS spectra of different concentrations of R6G adsorbed onto Ag MFs film, the SERS spectra of the R6G decreased with the reducing concentration. Many main peaks still can be distinctly detected in the spectra as the R6G concentration was down to 10^{-7} M, demonstrating the high sensitivity of the Ag MFs film. Thus, the Ag MFs film is both an excellent candidate for SERS substrate and catalysis.

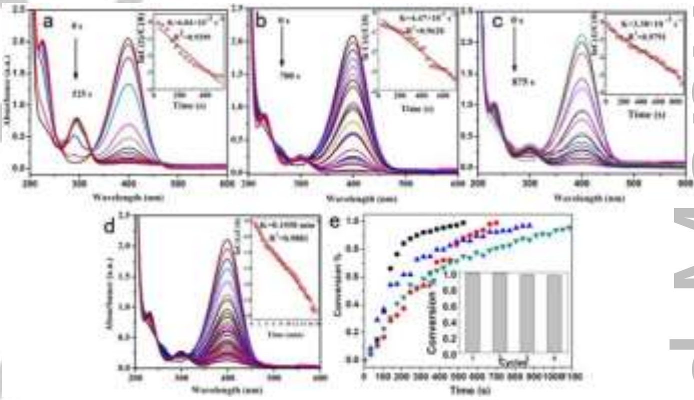

Figure 5. UV-vis absorption spectra of the reduction of 4-NP by $NaBH_4$ catalyzed by the Ag MFs film for recorded for the (a)1st, (b) 2nd, (d) 3rd, (d) 4th, (Insets: The corresponding plots of ln(C(t)/C(0)) versus reaction time for the reduction of 4-NP.)

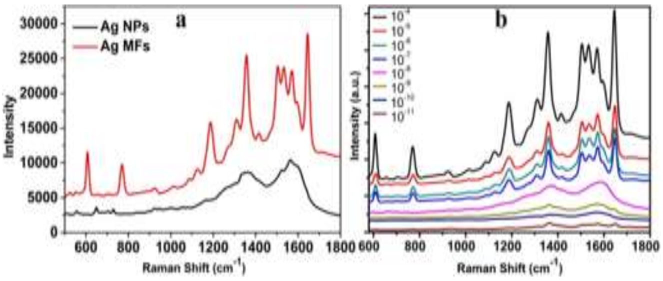

Figure 6. SERS spectra of R6G obtained by dropping 10 μL R6G ethanol solution (a) on Ag NPs and Ag MFs with 10^{-4} M R6G, (b) with different concentrations of R6G (10^{-4}-10^{-11} M) on Ag MFs substrate.

Conclusions

In summary, three-dimensional flower like Ag MFs films were fabricated, the growth mechanism of flower like Ag microstructures was also investigated by SEM, indicated the morphology and size of the Ag micro-flowers can be easily controlled by varying the reaction time. This technique provides great flexibility in tuning the shapes of Ag micro-flower on the film. Significantly catalytic activity and reusability demonstrates that the Ag MFs film is an excellent candidate for high active catalyst. The Ag MFs film exhibited obvious enhancement signals with all concentrations of R6G solutions, and the main Raman bands were still visible even at a concentration as low as10^{-7} M. Therefore, the Ag MFs film exhibited great potentials in catalysis and SERS applications.

Experimental Section

Materials

All chemicals are of analytical purity and used without further purification. $HAuCl_4 \cdot 3H_2O$ (99.99 %) and (3-aminopropyl) trimethoxysilane (APTMS) were purchased from Sigma (USA), p-dihydroxybenzene (98 %) and $AgNO_3$ (99.8 %) were obtained from Beijing Chemical Reagents (Beijing, P. R. China). R6G was purchased from Aladdin (Shanghai, P. R. China). All other reagents were used as received.

Fabrication of nanosheets-assembled Ag micro-flowers (Ag MFs) film

The glass and silicon slices as substrates were first treated in a Piranha cleaning solution (70% sulphuric acid/ 30% hydrogen peroxiden), then rinsed with ultrapure water and soaked in an ethanol solution of 1 % APTMS for 20 min. The substrates were rinsed thrice by ethanol and ultrapure water to remove the APTMS solution, and then dried in flowing nitrogen prior to use. The APTMS modified glass and silicon slices were soaked in a colloid dispersion of Au NPs with diameter of 15 nm (the synthesis of Au NPs was provided in supporting information) for 15 min, and rinsed with ultrapure water to remove the unstuck Au NPs. Then the Au NPs substrates were immersed into a mixture solution containing 2 mL of $AgNO_3$ (100 mM), 30 mL of hydroquinone (0.5 M) and 10 mL of citrate buffer (pH=3.5-3.8) for 1 min-8 min at room temperature, and then rinsed with enough tap water. After dried at 50 ˚C, the Ag flower film was prepared. The Raman spectra of R6G with different concentrations (10^{-4} M-10^{-10} M) were collected by dropping a 10 μL of ethanol solution of R6G on the Ag MFs film fabricated on silicon wafer.

Catalysis

For the catalytic reduction of 4-NP, aqueous solutions of 4-NP (0.01 M, 0.03 mL) and NaBH4 (0.5 M, 0.2 mL fresh prepared by ice water) solution were mixed with water (2.5 mL) in a quartz cuvette without stirring. Then a slice of Ag MFs on glass substrate was added as catalyst, meanwhile, the reaction process was monitored by UV-vis spectroscopy. Kinetic results obtained from UV-vis spectra with various time intervals. Similarly, the Ag MFs substrate were explored as a catalyst for the reduction of 4-NTP. The results of 4-NP and 4-NTP in the reduction of reaction were displayed in Table S1.

Characterization

The Scanning electron microscopy (SEM) images and energy-dispersive X-ray spectroscopy (EDS) analysis were performed with a Hitachi Su-70 electron microscope. The UV–vis spectroscopy was recorded with a UV-2600 spectrophotometer (Shimadzu, Japan). The Surface-enhanced Raman measurements were recorded by a Raman microscope (Princeton Instruments (HORIBA HR800)) with an excitation laser wavelength of 488 nm.

Acknowledgements

The authors gratefully acknowledge the financial support from the National Natural Science Foundation of China (Project No. 21205024), the National Science Foundation for Post-doctoral Scientists of China (Grant No. 2012M520659, 2013T60307).

Keywords: sliver • flower like structure• film • catalysis • Surface-enhanced Raman scattering

[1] D. Yang, X. Liu, C. P. Teng, C. Owh, K. Y. Win, M. Lin, X. J. Loh, Y. Wu, Z. Li and E. Ye, *Nanoscale*, **2017**, *9*, 15753-15759.
[2] Y. N. Xia, K. D. Gilroy, H. C. Peng and X.H. Xia, *Angew.Chem.Int. Ed*. **2017**, *56*, 60-95.
[3] C. H Moran, M. Rycenga, X. H. Xia, C. M. Cobley and Y. N. Xia, N*anotechnology*, **2014**, *10*, 014007.
[4] X. Wang, A. Ruditskiy, Y. N. Xia, *Natl. Sci. Rev.*, **2016**, *3*, 520-533.
[5] Y. Zhang, J. Liu, J. Ahn, T. Xiao, Z. Y. Li and D. Qin, *ACS Nano*, **2017**, *11*, 5080-5086.
[6] T. Huang, H.M. Li, L. Huang, S.L. Li, K. Li, Y. F. Zhou, *Langmuir*, **2016**, *32*, 991-996.
[7] A. C. Muhammed, K. P. Faseela, S. Singh, S. Baik, *Scientific Reports*, 2016, *6*, 34894.
[8] A. G. M. Silva, T. S. Rodrigues, S. J. Haigh and P. H. C. Camargo, *Chem. Commun*. **2017**, *53*, 7135-7148.
[9] S. D. Nie, C.Y. Liu, Z. Y. Zhang, Y. Liu, *RSC Adv***.**, 2016, **6**, 21511-21516.
[10] M. Xu, Y. M. Sui, C. Wang, B. Zhou, Y.J. Wei, B. Zou, *J. Mater. Chem. A***,** **2015**, *3*, 22339-22346.
[11] Y. H. Chang, C. Liu, S.G. Rouvimov, T.F. Luo and S. P. Feng, *Chem. Commun*. **2017**, *53*, 6752-6755.
[12] Y. H. You, Y. W. Lin and C. Y. Chen, *RSC Adv*. **2015**, *5*, 93293-93300.
[13] K. Nabeela, R. T. Thomas, J. B. Nair, K. K. Maiti, K. G. K. Warrier and S. Pillai, *ACS Appl. Mater. Interfaces*, **2016**, *8*, 29242–29251.
[14] C. W. Wang, J. F. Wang, P. Li, Z. Rong, X. F. Jia, Q. L. Ma, R. Xiao and S. Q. Wang, *Nanoscale*, **2016**, *8*, 19816-19828.
[15] P. Xu, L. L. Kang, N. H. Mack, K. S. Schanze, X. J. Han, H. L. Wang, S*cientific Reports*, **2017**, *3*, 2997.
[16] P. Xu, B. Zhang, N. H. Mack, S. K. Doorn, X. J. Han, H. L. Wang, *J. Mater. Chem.*, **2010**, *20*, 7222-7226.
[17] P. Xu, X. J. Han, B. Zhang, Y. C. Du and H. L. Wang, *Chem. Soc. Rev.*, **2014**, *43*, 1349-1360.
[18] Q. D. Xia, D. Y. Su, X. Yang, F. Chai, C. G. Wang and J. J. Jiang, *RSC Adv*. **2015**, *5*, 58522-58527.
[19] Q. D. Xia, S. S. Fu, G. G. Ren, F. Chai, J. J. Jiang and F. Y. Qu, *RSC Adv*. **2016**, *6*, 55248-55256.
[20] K. H. Zhang, C. W. Wang, Z. Rong, R. Xiao, Z. Zhou and S. Q. Wang, *New J. Chem*. **2017**, *41*, 14199-14208.
[21] B. Seo, S. Choi and J. W. Kim, *ACS Appl. Mater. Interfaces*, **2011**, *3*, 441-446.
[22] Y. Wu, T. Hang, J. Komadina, H. Ling and M. Li, *Nanoscale*, **2014**, *6*, 9720-9726.
[23] M. Rajab, K. Mougin, M. Derivaz, L. Josien, V. Luchnikov, J. Toufaily, K. Hariri, T. Hamieh, R. Lohmus, H. Haidara, Colloids and Surfaces A: Physicochem. Eng. Aspects, **2015**, *484*, 508-517.
[24] S. Li, T. Wei, M. Y. Tang, F. Chai, F.Y. Qu, C.G. Wang, *Sensors and Actuators B: Chemical*, **2018**, *255*, 1471-1481.
[25] H. B. Tang, P. Zheng, G.W. Meng, Z.B. Li, C.H. Zhu, F.M. Han, Y. Ke, Z.M. Wang, F. Zhou and N. Q. Wu, *Nanotechnology*, **2016**, *27*, 325303.

[26] Y. Zhao, X.Y. Li, L.C. Zhang, B. H. Chu, Q.Y. Liu and Y. L. Lu, *RSC Adv.*, **2017**, *7*, 49303-49308.

[27] S. Wang, S.Y. Song, R. P. Deng, H. L. Guo, Y. Q. Lei, F. Cao, X. Y. Li, S. Q. Su and H. J. Zhang, *CrystEngComm*, **2010**, *12*, 3537-3541.

[28] T. H. JAMES, *J. Am. Chem. Soc*., **1939**, *61*, 648–652.

[29] A. G. M. D. Silva, T. S. Rodrigues, S. J. Haigh and P. H. C. Camargo, *Chem. Commun.* **2017**, *53*, 7135-7148.

[30] Q.F. Zhang, Y.D. Zhou, E. Villarreal, Y. Lin, S. L. Zou and H. Wang, *Nano Lett.* **2015**, *15*, 4161-4169.

[31] Wu, D. Su and D. Qin, *ChemNanoMat*, **2017**, *3*, 245-251.

[32] J. Li, Y. Wu, X. Sun, J. Liu, S. A. Winget and D. Qin, *Chem.Nano.Mat*, **2016**, *2*, 786-790.

[33] S. S. Fu, G. J. Ren, S. Li, F. Chai, C. G. Wang and F. Y. Qu, *New J. Chem.*, **2017**, *41*, 1509-1517.

[34] H. T. Wang, Z. X. Dong and C. Z. Na, *ACS Sustainable Chem. Eng*. **2013**, *1*, 746-752.

Entry for the Table of Contents (Please choose one layout)

Layout 1:

FULL PAPER

Text for Table of Contents

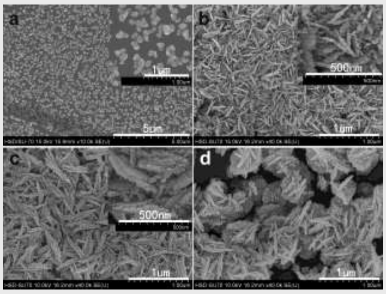

Key Topic*

*Qijun Dai,[a,b], Lu Li,[a] Chungang Wang,[a] Changli Lv, *[a] Zhongmin Su*[a] and Fang Chai *[a,b]*

Page No. – Page No.

Fabrication of flower like Ag microspheres film with its application in catalysis and as SERS substrates

*Flower like Ag microstructures film with its application in catalysis and SERS.